

Submitted to the
XXXIII International Conference on High Energy Physics
July 26 - August 2, 2006, Moscow, Russia

Abstract:

Session: Beyond the Standard Model

Search for High- P_T Isolated Leptons with ZEUS at HERA

ZEUS Collaboration

Abstract

A search for events with isolated high transverse energy leptons and large missing transverse momentum has been performed with the ZEUS detector at HERA using data samples with a total integrated luminosity of 249 pb^{-1} taken during the 1998-2005 running period. The results are compared to the Standard Model predictions and the efficiencies of ZEUS and H1 at HERA for finding such events are discussed.

1 Introduction

This paper reports the results of an investigation of the production of isolated leptons in events with a topology matching the electron¹ or muon decay channel of singly produced W bosons in electron-proton collisions at a centre-of-mass energy of 318 GeV. Single W production is a rare Standard Model (SM) process and an important source of background to searches for physics beyond the Standard Model at HERA [1, 2]. Investigations of the process $ep \rightarrow eWX, W \rightarrow l\nu$, where $l = \mu, e, \tau$, have been performed at HERA by both the H1 [2–4] and ZEUS [1, 5–8] collaborations. The H1 collaboration observes an excess of events with isolated muons or electrons, high missing transverse momentum and large values of hadronic transverse momentum over the SM prediction, dominated by single W production. The ZEUS results based on searches for isolated electrons and muons at a centre-of-mass energy of 300 GeV and 318 GeV do not confirm this excess. The search described completes the 1998-2005 ZEUS data set for both electron and muon channels, and the isolated muon search is more closely comparable to the H1 analysis than previous ZEUS searches. The ZEUS and H1 detector sensitivities differ in some kinematic regions due to their individual angular acceptance. The efficiencies of the two detectors for finding electrons or muons from single W production are compared in section 7 to investigate if the excess seen by H1 occurs in a kinematic region to which ZEUS is not sensitive.

The dominant leading order Feynman diagrams for single W production at HERA are shown in Fig. 1. In the leptonic decay-channel of the W , events typically contain an isolated lepton with high transverse momentum, P_T^l , and missing total transverse momentum, P_T , arising from the escaping neutrino. If the negative of the four-momentum transfer squared (Q^2) is greater than a few GeV², the scattered electron can be observed in the detector.

The study was performed by selecting events containing isolated electrons or muons with high P_T^l , in events with large missing P_T . The data set corresponds to the 1998-99 e^-p and 1999-2000 e^+p running period, with total integrated luminosities of 17 and 66 pb⁻¹, respectively (HERA-I) and the running periods 2003-04 e^+p and 2004-05 e^-p with total integrated luminosities of 40 pb⁻¹ and 126 pb⁻¹, respectively (HERA-II). For the decay channel of the W into electrons only the e^-p data sets from HERA-I and II are presented here, as the results for the e^+p running periods have been shown previously [8]. In all running periods the centre-of-mass energy was 318 GeV.

¹ In this paper “electron” refers both to electrons and positrons unless specified.

2 Monte Carlo simulation of the signal $e^\pm p \rightarrow e^\pm W X$ and of the background

The leading order (LO) cross section for $e^\pm p \rightarrow e^\pm W X$ has been calculated using the EPVEC generator [9]. EPVEC calculates the cross section in two regions, corresponding to photoproduction and deep inelastic scattering, which are separated by a cut on the variable u , defined as $(p_q - p_W)^2$, where p_q and p_W are the 4-momenta of the initial state quark and of the W, respectively. The photon (proton) structure functions used in the calculation are GRV-G(LO) (CTEQ5D). The final state simulation does not include hard gluon radiation.

Such calculations yield a total cross section of 1.1 pb for $\sqrt{s} = 318$ GeV. The uncertainties on this value are approximately 5% for the choice of $|u_{\text{cut}}|$ (set at 25 GeV^2), 5% for the choice of proton structure function, 10% for the choice of photon structure function and 10% from the choice of Q^2 scale [10] used in EPVEC. Next-to-leading order corrections have been calculated [11] and were found to be of the order of 10%; they were however neglected in this analysis.

The most important background to W production in the electron decay-channel arises from high Q^2 charged and neutral current deep inelastic scattering (DIS) events. These DIS events have been simulated using the generator DJANGO6 [12], an interface to the Monte Carlo (MC) programs HERACLES 4.5 [13] and LEPTO 6.5 [14]. Leading order electroweak radiative corrections were included and higher order QCD effects were simulated using the colour-dipole model (CDM) of ARIADNE [15] or using a leading-logarithm approximation (MEPS). The hadronisation of the partonic final state was performed by JETSET [16]. Two-photon processes which are a minor contribution to the background of the electron channel of W boson decay but are the most important background in the muon channel were simulated using the GRAPE [17] dilepton generators. Direct and resolved photoproduction processes were simulated using the HERWIG 6.1 [18] event generator but they are found not to contribute after the event pre-selection.

The generated events were passed through the GEANT-based [19] ZEUS detector and trigger simulation programs [20]. They were reconstructed and analysed by the same program chain as the data.

3 The ZEUS detector

A detailed description of the ZEUS detector can be found elsewhere [20]. The main components used in this analysis were the compensating uranium-scintillator calorimeter

and the central tracking detector.

The high-resolution uranium–scintillator calorimeter (CAL) [21] consists of three parts: the forward (FCAL), the barrel (BCAL) and the rear (RCAL) calorimeters. Each part is subdivided transversely into towers and longitudinally into one electromagnetic section (EMC) and either one (in RCAL) or two (in BCAL and FCAL) hadronic sections (HAC). The smallest subdivision of the calorimeter is called a cell. The CAL energy resolutions, as measured under test-beam conditions, are $\sigma(E)/E = 0.18/\sqrt{E}$ for electrons and $\sigma(E)/E = 0.35/\sqrt{E}$ for hadrons (E in GeV).

Charged particles are tracked in the central tracking detector (CTD) [22], which operates in a magnetic field of 1.43 T provided by a thin superconducting coil. The CTD consists of 72 cylindrical drift chamber layers, organised in 9 superlayers covering the polar-angle² region $15^\circ < \theta < 164^\circ$.

A three-level trigger was used to select events online [23] requiring large missing P_T .

4 Event Reconstruction and Data Preselection

The missing transverse momentum is defined as:

$$P_T = \sqrt{\left(\sum_i p_{X,i}\right)^2 + \left(\sum_i p_{Y,i}\right)^2},$$

where $p_{X,i} = E_i \sin \theta_i \cos \phi_i$ and $p_{Y,i} = E_i \sin \theta_i \sin \phi_i$ are calculated from individual energy deposits in clusters of calorimeter cells corrected [24] for energy loss in inactive material. The angles θ_i and ϕ_i are estimated from the geometric cell centres and the event vertex. In $W \rightarrow e\nu$ events, P_T as defined above is an estimate of the missing transverse momentum carried by the neutrino. In $W \rightarrow \mu\nu$ events the muon as a minimum ionising particle deposits very little energy in the calorimeter and therefore a better estimate of the transverse momentum carried by the neutrino can be obtained if the momentum of the muon is calculated from the muon track measured in the central tracking detector. Combining with the above estimate of the total transverse momentum from the calorimeter, it leads to:

$$P_T^{\text{miss}} = \sqrt{\left(\sum_i p_{X,i}^{\text{CAL}} + p_X^{\mu,\text{track}}\right)^2 + \left(\sum_i p_{Y,i}^{\text{CAL}} + p_Y^{\mu,\text{track}}\right)^2}.$$

² The polar-angle is defined relative to the Z axis of the ZEUS co-ordinate system which is a right-handed Cartesian system, with the Z axis pointing in the proton beam direction, referred to as the “forward direction”, and the X axis pointing left towards the centre of HERA.

Hadron transverse momenta P_T^X are defined as sums over those calorimeter cells that are not assigned to lepton candidate clusters. The electron transverse momentum P_T^e was calculated from the calorimeter cluster associated with the electron, whereas the muon transverse momentum was calculated entirely from the track information. Longitudinal momentum conservation ensures that $E - p_z$ (δ), defined as:

$$\delta \equiv \sum_i E_i(1 - \cos \theta_i),$$

peaks at twice the electron beam energy $E_e = 27.5$ GeV for fully contained events. Small values of δ are expected for proton-gas interactions. Values much greater than $2E_e = 55$ GeV are usually caused by the superposition of a neutral current DIS event with additional energy deposits in the RCAL not related to ep collisions. Only events with $5 < \delta < 60$ GeV for the electron channel and with $\delta < 70$ GeV for the muon channel were chosen in the preselection.

The acoplanarity angle ϕ_{ACOP} , illustrated in Fig.2, is the azimuthal separation of the outgoing lepton and the vector in the $\{X, Y\}$ plane that balances the hadronic- P_T vector. For well measured neutral current events, the acoplanarity angle is close to zero, while large acoplanarity angles indicate large missing energies.

The transverse mass is defined as:

$$M_T = \sqrt{2P_T^l P_T^\nu (1 - \cos \phi^{l\nu})},$$

where P_T^l is the lepton transverse momentum, P_T^ν is the magnitude of P_T and $\phi^{l\nu}$ is the azimuthal separation of the lepton and the P_T vectors as shown in Fig. 2.

The quantity ξ_e^2 is defined as

$$\xi_e^2 = 2E'_e E_e (1 + \cos \theta_e),$$

where E'_e is the energy of the final state electron and θ_e is the polar angle of the electron measured in the calorimeter. For neutral current events, where the scattered electron is identified as the isolated lepton, this quantity corresponds to the virtuality, Q^2 . Neutral current events will generally have low values of ξ_e^2 whilst electrons from W decay will generally have high values of ξ_e^2 .

Events that passed the trigger requirements were further required to have P_T greater than 12 GeV. The transverse momentum calculated excluding the inner ring of calorimeter cells around the forward beam pipe hole, also had to be greater than 9 GeV. These offline cuts were more stringent than the corresponding online trigger thresholds. Other pre-selection cuts were the requirement that the Z -coordinate of the tracking vertex be reconstructed within 50 cm of the nominal interaction point and that there was a track from the vertex

associated with the lepton, whereas for events from the HERA-II running period this track was required to reach at least the third inner superlayer of the CTD ($0.32 < \theta < 2.80$ rad as viewed from the nominal interaction point). In addition, since most fake leptons are misidentified hadrons close to jets, the background was further reduced by requiring that the lepton track be separated by at least 0.5 units in $\{\eta, \phi\}$ space from other tracks associated with the event vertex with momentum larger than 0.2 GeV, where ϕ is the polar angle and $\eta \approx -\log(\tan(\theta/2))$. In HERA-II the tracks used in this track-isolation requirement were required to pass at least the third inner superlayer of the CTD. Cuts on the calorimeter timing and algorithms based on the pattern of tracks rejected beam-gas, cosmic-ray and halo-muon events.

After these preselection criteria were applied, events with isolated electrons and isolated muons were selected separately as described in the following sections.

5 Search for isolated electrons

An algorithm that selects candidate electromagnetic clusters in the calorimeter and combines them with tracking information was used to identify electrons. It was optimised for maximum electron-finding efficiency and electron-hadron separation for neutral current DIS events [25, 26]. The electromagnetic cluster energy was required to be > 8 GeV. The impact point at the face of the calorimeter was determined with a resolution of 1 cm using the pulse height information from the pairs of photomultipliers reading out each cell. The distance of closest approach of the closest extrapolated track to the electromagnetic cluster was required to be less than 10 cm. The background from fake electrons was reduced by requiring that the energy not associated with the electron in an $\{\eta, \phi\}$ cone of radius 0.8 around the electron direction be less than 4 GeV.

The data events are compared to the expectation from the Monte Carlo simulation in Fig. 5 and Fig. 6, after requiring that the P_T^e be greater than 5 GeV, the transverse mass M_T be greater than 10 GeV, that the quantity δ lie in the range $5 < \delta < 60$ GeV and that θ_e be less than 2.0 rad. Neutral current background events dominate the sample at this stage of the selection, as is evident from the steeply falling P_T spectrum and the concentration of events at small acoplanarity angles. A Jacobian peak structure is visible in the transverse mass distribution for the Monte Carlo simulation of the signal events.

In the final selection the neutral current background was strongly suppressed by further requiring δ to be less than 50 GeV and the acoplanarity angle to be greater than 0.3 rad for events which have a hadronic transverse momentum, P_T^X , larger than 4 GeV (otherwise no acoplanarity angle cut is applied). In addition for low values of P_T (< 25 GeV), where neutral current events dominate, ξ_e^2 was required to be greater than 5000 GeV². Electrons

in the final event sample were required to have $P_T^e > 10 \text{ GeV}$ and $\theta_e < 1.5 \text{ rad}$. Finally, requiring that the matching electron track have a transverse momentum greater than 5 GeV removed most of the remaining fake electrons.

Seven data events, only one from the HERA-I sample, passed these final cuts in the $P_T^X > 12 \text{ GeV}$ region. The expectation from the SM and the fraction arising from the single W production MC, in bins of P_T^X , are given in Table 1 together with the numbers observed in similar searches by the H1 collaboration [2, 27, 28] and previous searches by the ZEUS collaboration [8]. The fraction of the SM prediction arising from the signal in e^-p collisions is lower than in e^+p due to the enhanced charged current DIS cross section. The signal contribution to the SM expectation for the whole 98-05 $e^\pm p$ data set is similar to that expected by H1. No excess over the Standard Model predictions is observed by ZEUS.

One of the events surviving the final selection is shown in Fig. 3.

The systematic effects on the background and signal expectations considered were:

- using CDM instead of MEPS for hadronisation in the background simulation;
- varying the absolute hadronic (electromagnetic) energy scale of the CAL by $\pm 3\%$ ($\pm 2\%$);
- varying the electron beam polarisation by $\pm 50\%$ around its value at -0.058 ;
- a systematic uncertainty on the integrated luminosity of 2.25% (5%) for the 1998-1999 (2004-5) running period.

Theoretical uncertainties on the W production cross section were not included in the errors on the SM prediction.

6 Search for isolated muons

For the search of $ep \rightarrow eWX$ with subsequent decay $W \rightarrow \mu\nu$ the sample of events preselected as described in section 4 with a large calorimeter missing P_T was used.

The energy deposited by minimum-ionising particles (MIPs) can be distributed across several calorimeter clusters. Therefore neighbouring clusters were grouped together into larger scale objects which, provided they passed topological and energy cuts, were assigned to calorimeter MIPs. In this analysis a muon candidate was selected as a calorimeter MIP matched to an extrapolated CTD track from the primary vertex to within 20 cm , where for HERA-II only tracks passing the third inner CTD superlayer were considered [29].

The muon transverse momentum, P_T^μ , and direction, including the polar angle θ_μ , were obtained from the matching track which was required to satisfy $P_T^\mu > 10 \text{ GeV}$ and $\theta_\mu < 2.0 \text{ rad}$

and to be isolated by at least 0.5 units in $\{\eta, \phi\}$ space from any jet with $E_T^{\text{jet}} > 5 \text{ GeV}$ and $-3 < \eta^{\text{jet}} < 3$. Events in which more than one muon with $P_T^\mu > 1 \text{ GeV}$ was found were rejected. In addition, the transverse mass M_T was required to be greater than 5 GeV and the quantity δ less than 70 GeV. The comparison between data and Monte Carlo expectation satisfying these requirements is shown in Fig. 7 for the 98-05 e^-p data set, in Fig. 8 for 99-04 e^+p and in Fig. 9 for the full 98-05 $e^\pm p$ data set.

In the final selection the acoplanarity angle was required to be greater than 0.2 rad. This cut significantly reduced the dilepton background. Finally, both the P_T^X and the total P_T from the CAL including the MIP's energy deposit had to be greater than 12 GeV.

Six data events survived the final cuts. One of the events surviving the final selection is shown in Fig. 4 and the comparison between data and Monte Carlo expectation for the final selection can be found in Figs. 10, 11 and 12 for the 98-05 e^-p , 99-04 e^+p and 98-05 $e^\pm p$ data sets, respectively. The expectation from the SM and the fraction arising from the single W production MC, in bins of P_T^X , are given in Table 2 together with the numbers observed in similar searches by the H1 collaboration [28]. The signal contribution to the SM expectation is similar to that expected by H1. No excess over the Standard Model predictions is observed by ZEUS.

The systematic effects on the background and signal expectations considered were the same as for the case of isolated electrons. Additionally, it was checked that beauty photoproduction does not contribute to the background expectation.

As in the case of the electrons, theoretical uncertainties on the W -production cross section were not included in the errors on the SM prediction.

7 Comparison of H1 and ZEUS Selection Efficiencies

The isolated lepton selections employed by the H1 [30] and ZEUS collaborations are optimised for their respective detectors. The main difference in the selections is due to the cut on the lepton polar angle, which is $5^\circ < \theta_l < 140^\circ$ for H1 and $17^\circ < \theta_e < 86^\circ$, $17^\circ < \theta_\mu < 115^\circ$ in the ZEUS analysis. Consequently, the sensitivity of the detectors to the decay products from single W production differs in some kinematic regions, which are defined in terms of the polar angle θ_l and the transverse momentum of the final state lepton P_T^l .

The efficiency of the two detectors was studied with a single W production Monte Carlo sample generated with EPVEC, using the respective event selections from the H1 and ZEUS analyses. The efficiency was defined as the number of reconstructed events passing the final selection divided by the number of generated events in the kinematic region $5^\circ < \theta_l < 140^\circ$ and $P_T^l > 10 \text{ GeV}$.

Figure 13 shows the H1 and ZEUS efficiencies for detecting electrons from single W decay as a function of P_T^X . The observed drop in the ZEUS efficiency in the lowest bin is due to the analysis cut $P_T^X > 12$ GeV. At large P_T^X the efficiencies are seen to be flat and more comparable. The arrows indicate the position of the observed data events. The bottom plot shows the efficiency as a function of θ_e at large hadronic transverse momentum $P_T^X > 25$ GeV, the kinematic region where an excess of data events is observed by H1 over the SM prediction. Here the cut $P_T^X > 25$ GeV is also made at the generator level. The θ_e distribution from EPVEC is also shown. It can be seen that in the common polar angle range the efficiencies of the H1 and ZEUS selection at large P_T^X are similar. Additionally, the majority of the H1 events observed at high P_T^X lie within this common region. The more limited angular range in the ZEUS analysis visible here is the main reason for the lower ZEUS efficiency visible at high P_T^X in the top plot.

The efficiencies in the muon channel are similarly displayed in Fig. 14. As observed in the electron channel, the efficiency as a function of P_T^X is found to be comparable between the H1 and ZEUS analyses and reasonably flat. It can also be seen that all six high P_T^X muon data events observed by H1 fall within the geometrical acceptance of the ZEUS selection.

8 Summary

A search was made for isolated high- P_T electrons and muons, in events with large missing P_T , compatible with single W production with decay in the electron and muon channel, respectively. The search was made in electron-proton collisions at centre-of-mass energy of 318 GeV using data samples with total integrated luminosity of 249 pb^{-1} . The rate of production of such events at high hadronic transverse momentum was found to be consistent with the Standard Model predictions. The excess in these type of events observed by the H1 collaboration is not confirmed whereas the efficiency of detecting electrons and muons from single W production at high P_T^X was found to be comparable between H1 and ZEUS.

References

- [1] ZEUS Coll., S. Chekanov et al., Phys. Lett. **B 559**, 153 (2003).
- [2] H1 Coll., V. Andreev et al., Phys. Lett. **B 561**, 241 (2003).
- [3] H1 Coll., C. Adloff et al., Eur. Phys. J. **C 5**, 575 (1998).
- [4] H1 Coll., *A search for events with isolated leptons and missing transverse momentum at HERA*. C. Veelken, presented at DIS2005, (2005).
- [5] ZEUS Coll., J. Breitweg et al., Phys. Lett. **B 471**, 411 (2000).
- [6] ZEUS Coll., S. Chekanov et al., Phys. Lett. **B 583**, 41 (2004).
- [7] ZEUS Coll., *Search for W production using the electron decay-channel in e^+p collisions at HERA I*. Abstract 3-0259, ICHEP2004, Beijing, China, (2004).
- [8] ZEUS Coll., *Search for events with high-PT isolated electrons and missing transverse momentum in ep collisions at HERA I and HERA II*. Abstract 257, *International Symposium on Lepton-Photon Interactions at High Energy, Uppsala, Sweden (LP2005)*, (2005).
- [9] U. Baur, J.A.M. Vermaseren and D. Zeppenfeld, Nucl. Phys. **B 375**, 3 (1992).
- [10] D. Waters, *'A First Estimate of $\sigma(e^+p \rightarrow e^+W^\pm X)$ and Studies of High P_T Leptons Using The ZEUS Detector*. Ph.D. Thesis, University of Oxford, (1998).
- [11] K-P. Diener, C. Schwanenberger and M. Spira, Eur. Phys. J. **C 25**, 405 (2002).
- [12] K. Charchula, G.A. Schuler and H. Spiesberger, Comp. Phys. Comm. **81**, 381 (1994).
- [13] A. Kwiatkowski, H. Spiesberger and H.-J. Möhring, Comp. Phys. Comm. **69**, 155 (1992). Also in *Proc. Workshop Physics at HERA*, 1991, DESY, Hamburg.
- [14] G. Ingelman, A. Edin and J. Rathsman, Comp. Phys. Comm. **101**, 108 (1997).
- [15] L. Lönnblad, Comp. Phys. Comm. **71**, 15 (1992).
- [16] T. Sjöstrand, Comp. Phys. Comm. **39**, 347 (1986).
- [17] T. Abe, Comp. Phys. Comm. **136**, 126 (2001).
- [18] G. Marchesini et al., Comp. Phys. Comm. **67**, 465 (1992).
- [19] R. Brun et al., GEANT3, Technical Report CERN-DD/EE/84-1, CERN, 1987.
- [20] ZEUS Coll., U. Holm (ed.), *The ZEUS Detector*. Status Report (unpublished), DESY (1993), available on <http://www-zeus.desy.de/bluebook/bluebook.html>.

- [21] M. Derrick et al., Nucl. Inst. Meth. **A 309**, 77 (1991);
 A. Andresen et al., Nucl. Inst. Meth. **A 309**, 101 (1991);
 A. Caldwell et al., Nucl. Inst. Meth. **A 321**, 356 (1992);
 A. Bernstein et al., Nucl. Inst. Meth. **A 336**, 23 (1993).
- [22] N. Harnew et al., Nucl. Inst. Meth. **A 279**, 290 (1989);
 B. Foster et al., Nucl. Phys. Proc. Suppl. **B 32**, 181 (1993);
 B. Foster et al., Nucl. Inst. Meth. **A 338**, 254 (1994).
- [23] ZEUS Coll., M. Derrick et al., Phys. Lett. **B 293**, 465 (1992).
- [24] ZEUS Coll., J. Breitweg et al., Eur. Phys. J. **C 11**, 427 (1999).
- [25] A. Kappes, *Verwendung Neuronaler Netze zur Identifikation des gestreuten Elektrons in ep-Ereignissen mit hohem Q^2 bei ZEUS*. Diploma Thesis, Universität Bonn, Bonn, Germany, Report BONN-IB-97-28, 1997, available on <http://www-zeus.physik.uni-bonn.de/german/diploma.html>.
- [26] ZEUS Coll., J. Breitweg et al., Z. Phys. **C 74**, 207 (1997).
- [27] H1 Coll., Integrated tables deduced from Phys. Lett **B 561**,241 with correct error propagation, available on <http://www-h1.desy.de/h1/www/publications/htmlsplit/DESY-02-224.long.html>.
- [28] H1 Coll., *Events with an isolated lepton and Missing Transverse Momentum at HERA*. J. Ferrando, presented at EPS 2005, Summer 2005, (2005), available on <http://www-h1.desy.de/h1/www/publications/htmlsplit/H1prelim-05-164.long.html>.
- [29] V. Kuzmin, for the ZEUS Coll., Nucl. Inst. Meth. **A 453**, 336 (2000).
- [30] H1 Coll., *Search for Events with Isolated Leptons and Missing Transverse Momentum*, 2006. Presented at ICHEP06.

| Isolated e candidates | $12 < P_T^X < 25$ GeV | $P_T^X > 25$ GeV |
|--|-------------------------|---------------------------------|
| ZEUS (prel.) 98-99 e^-p (17 pb $^{-1}$) | 1/0.23 \pm 0.06(67%) | 0/0.32 \pm 0.09(65%) |
| ZEUS (prel.) 04-05 e^-p (126 pb $^{-1}$) | 3/1.75 \pm 0.36 (57%) | 3/2.54 \pm 0.46 (51%) |
| ZEUS (prel.) 99-00 e^+p (66 pb $^{-1}$) | 1/1.04 \pm 0.11(57%) | 1/0.92 \pm 0.09(79%) |
| ZEUS (prel.) 03-04 e^+p (40 pb $^{-1}$) | 0/0.46 \pm 0.10(64%) | 0/0.58 $^{+0.08}_{-0.09}$ (76%) |
| ZEUS (prel.) 98-05 e^-p (143 pb $^{-1}$) | 4/1.98 \pm 0.36(58%) | 3/2.86 \pm 0.46(53%) |
| ZEUS (prel.) 99-04 e^+p (106 pb $^{-1}$) | 1/1.50 \pm 0.15(59%) | 1/1.50 $^{+0.12}_{-0.13}$ (78%) |
| ZEUS (prel.) 98-05 $e^\pm p$ (249 pb $^{-1}$) | 5/3.5 \pm 0.4(58%) | 4/4.4 \pm 0.5(61%) |
| H1 (prel.) 1994-2006 $e^\pm p$ (341 pb $^{-1}$) | - | 12/6.1 \pm 1.1(66%) |

Table 1: Summary of the results of searches for events with isolated electrons and missing transverse momentum at HERA. The number of observed events is compared to the SM prediction (observed/expected). The signal component of the SM expectation (W production) is given as a percentage in parentheses. The quoted errors contain statistical and systematic uncertainties added in quadrature. Only the H1 results directly comparable to the ZEUS results are quoted in this table.

| Isolated μ candidates | $12 < P_T^X < 25$ GeV | $P_T^X > 25$ GeV |
|---|------------------------|------------------------|
| ZEUS (prel.) 98-99 e^-p (17pb $^{-1}$) | 0/0.2 \pm 0.02 (67%) | 0/0.2 \pm 0.04 (85%) |
| ZEUS (prel.) 04-05 e^-p (127pb $^{-1}$) | 2/1.4 \pm 0.2 (68%) | 2/1.4 \pm 0.2 (86%) |
| ZEUS (prel.) 99-00 e^+p (66pb $^{-1}$) | 0/0.7 \pm 0.1 (72%) | 1/0.9 \pm 0.2 (79%) |
| ZEUS (prel.) 03-04 e^+p (40pb $^{-1}$) | 1/0.5 \pm 0.1 (64%) | 0/0.6 \pm 0.1 (82%) |
| ZEUS (prel.) 98-05 e^-p (144pb $^{-1}$) | 2/1.6 \pm 0.2 (68%) | 2/1.6 \pm 0.2 (86%) |
| ZEUS (prel.) 99-04 e^+p (106pb $^{-1}$) | 1/1.2 \pm 0.1 (69%) | 1/1.5 \pm 0.2 (80%) |
| ZEUS (prel.) 98-05 $e^\pm p$ (250pb $^{-1}$) | 3/2.8 \pm 0.2 (68%) | 3/3.1 \pm 0.3 (83%) |
| H1 (prel.) 1994-2006 $e^\pm p$ (341pb $^{-1}$) | - | 6/5.4 \pm 0.9 (77%) |

Table 2: Summary of the results of searches for events with isolated muons and missing transverse momentum at HERA. Other details as in table 1.

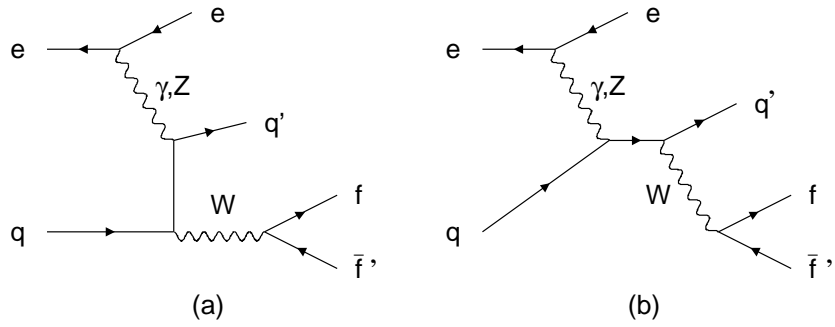


Figure 1: Main leading order Feynman diagrams for the process $ep \rightarrow eWX$.

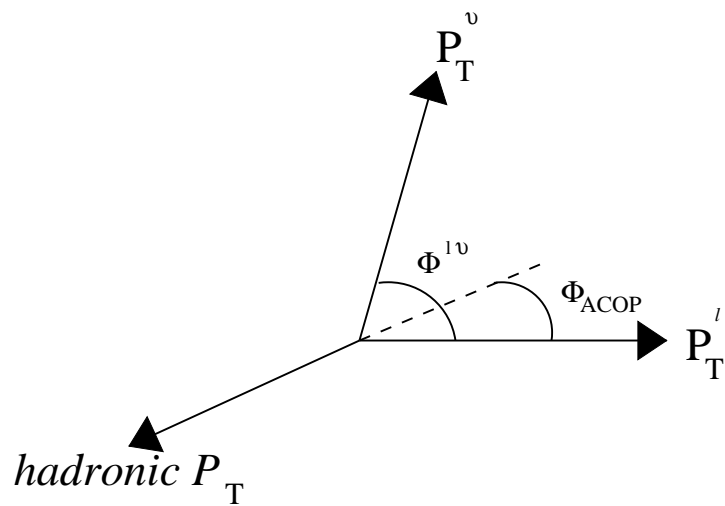


Figure 2: The definition of the acoplanarity angle, Φ_{ACOP} , and the azimuthal separation of the neutrino and the outgoing lepton, $\Phi^{l\nu}$, in the transverse plane. The dashed line balances the hadronic \mathbf{P}_T .

ZEUS

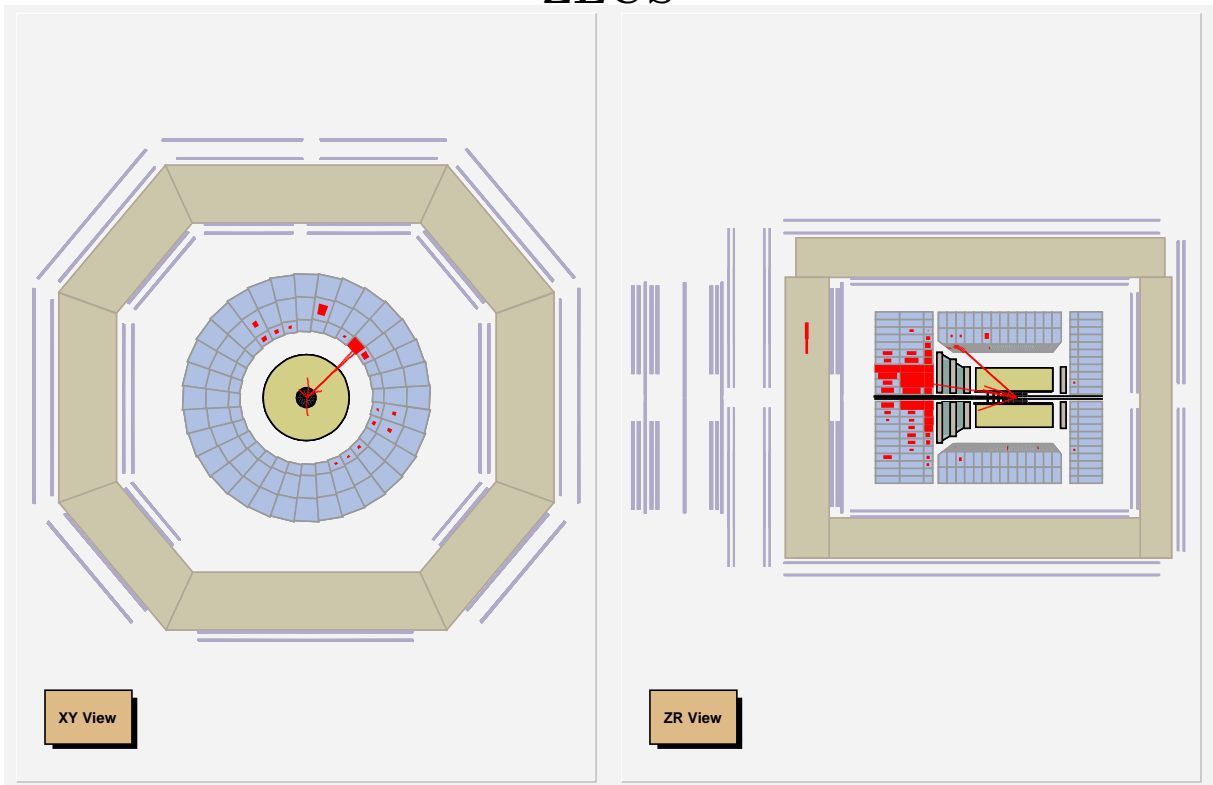


Figure 3: *Isolated electron candidate in an event with $P_T^X = 62$ GeV.*

ZEUS

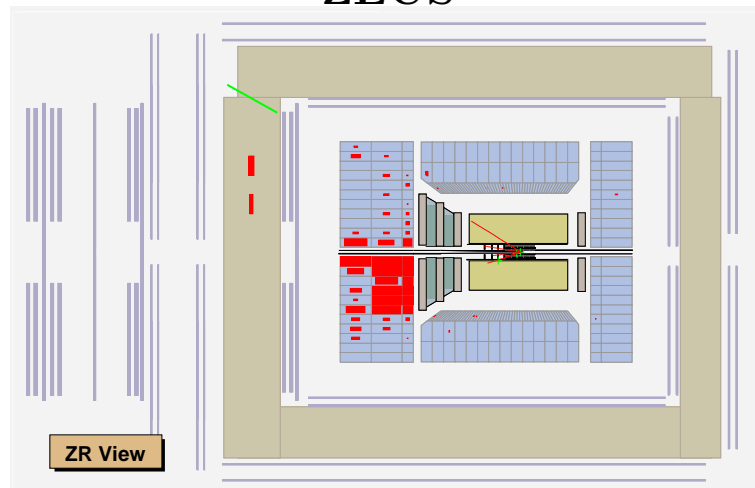


Figure 4: *Isolated muon candidate in an event with $P_T^X = 82$ GeV and missing $P_T = 77$ GeV.*

ZEUS

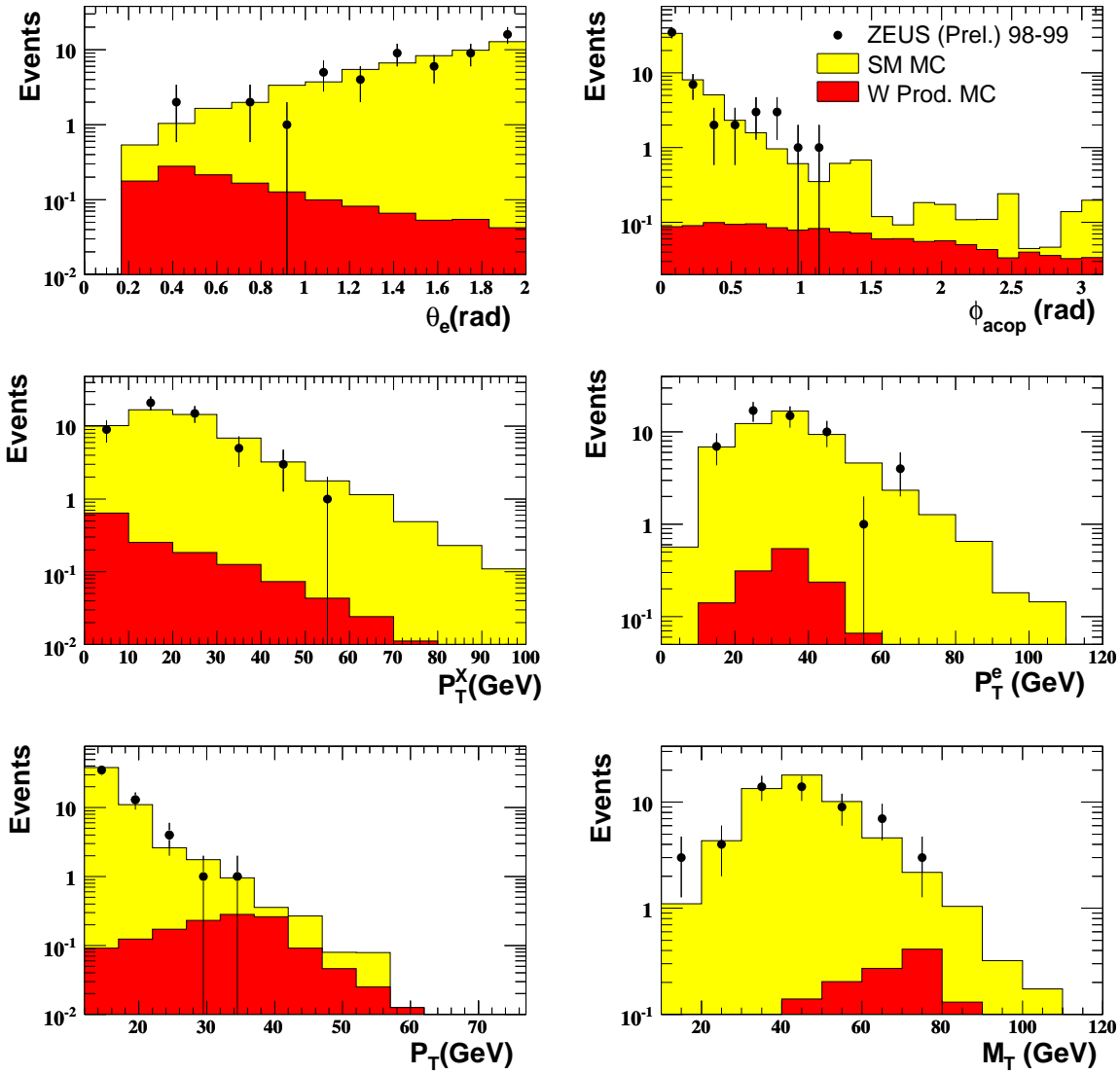


Figure 5: Isolated electron data (points) compared to absolutely-normalised Monte Carlo for the 1998-99 e^-p running period after the initial event selection. The light shaded histogram represents the Standard Model (SM) MC prediction, the dark shaded area the signal ($ep \rightarrow eWX$) prediction. The variables shown are described in detail in the text.

ZEUS

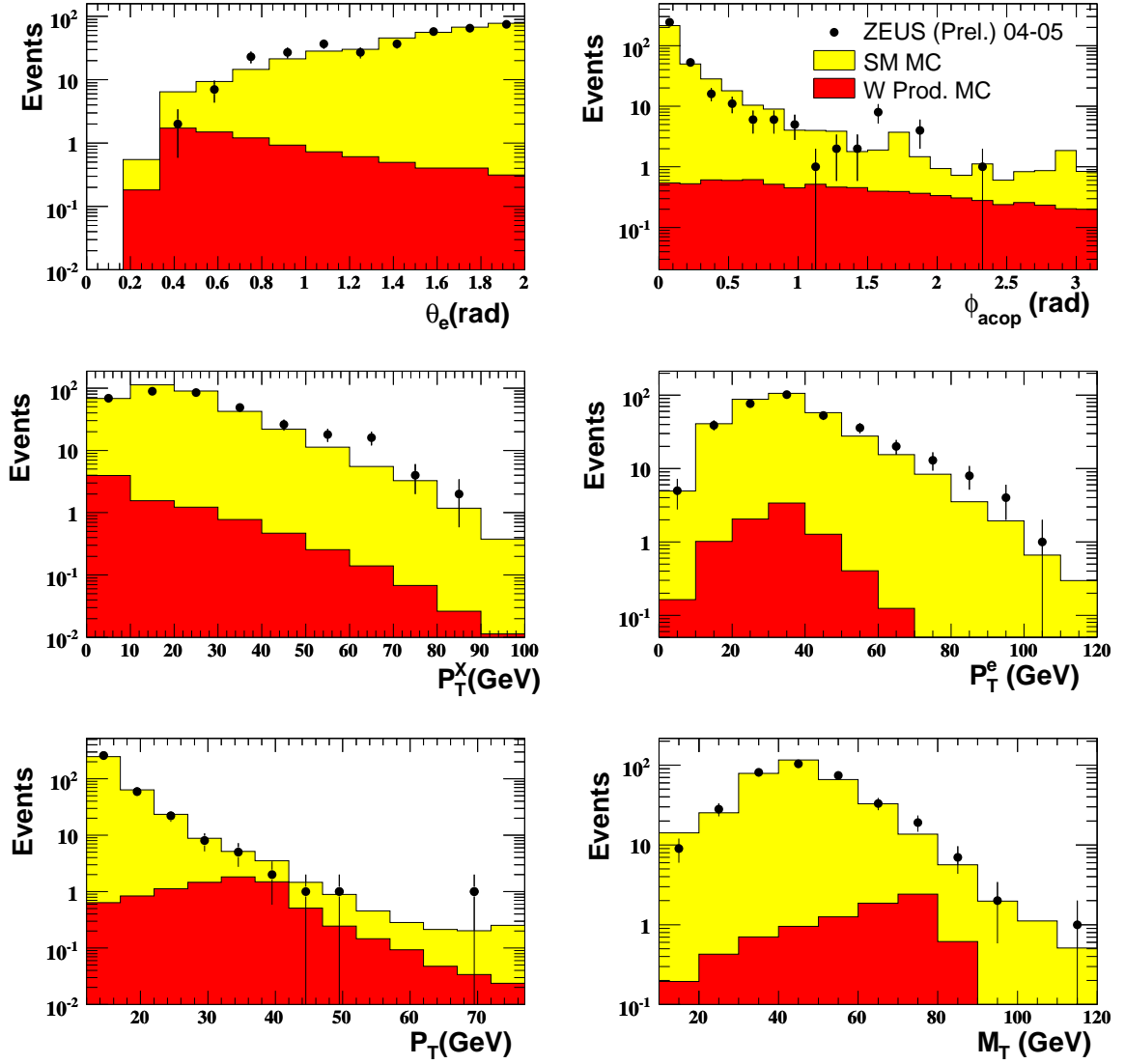


Figure 6: Isolated electron data (points) compared to absolutely-normalised Monte Carlo for the 2004-05 e^-p running period after the initial event selection. Other details as in Fig. 5.

ZEUS

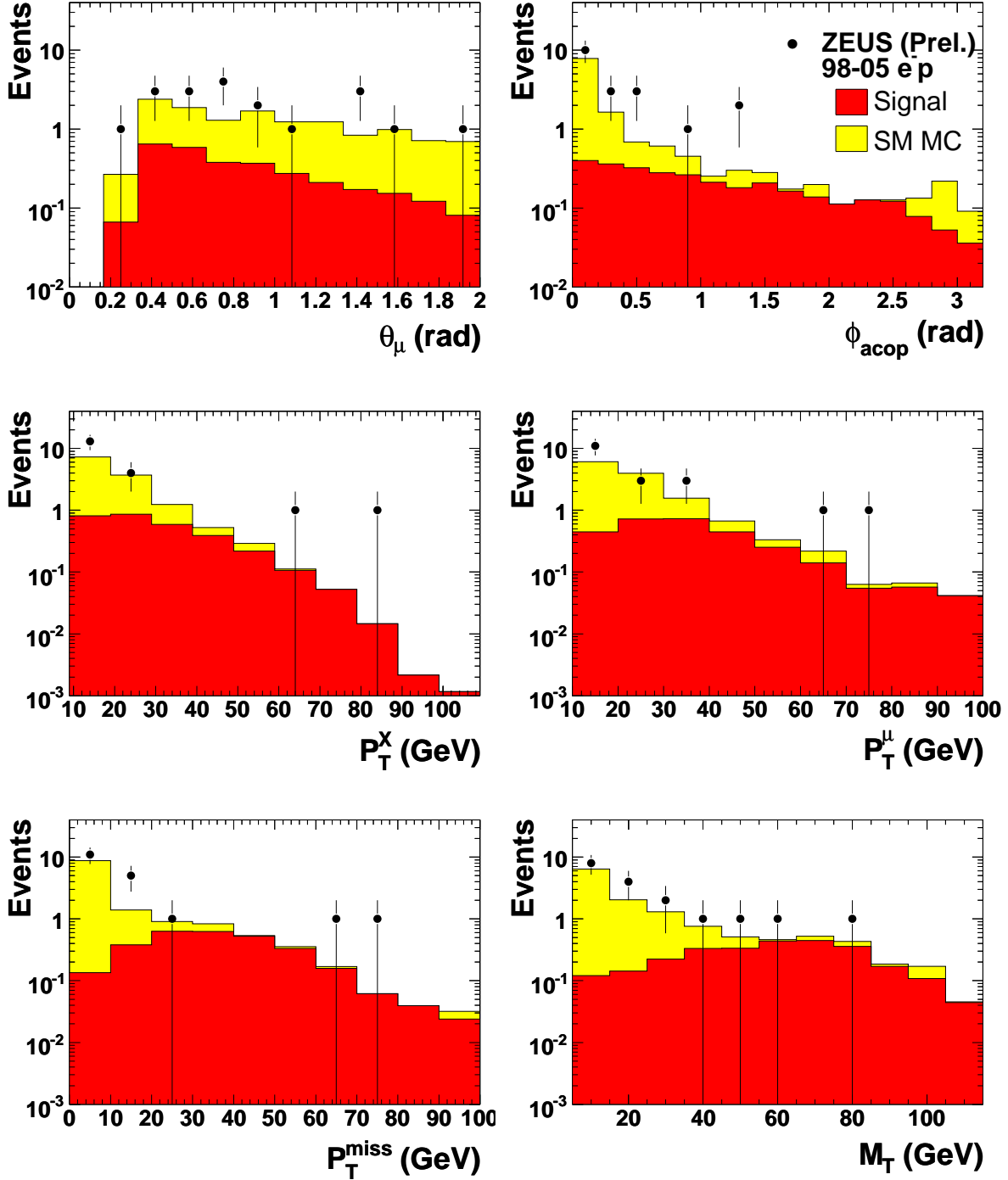


Figure 7: Isolated muon data (points) compared to absolutely-normalised Monte Carlo for the 1998-99, 2004-05 e^-p running period after the initial event selection. Other details as in Fig. 5.

ZEUS

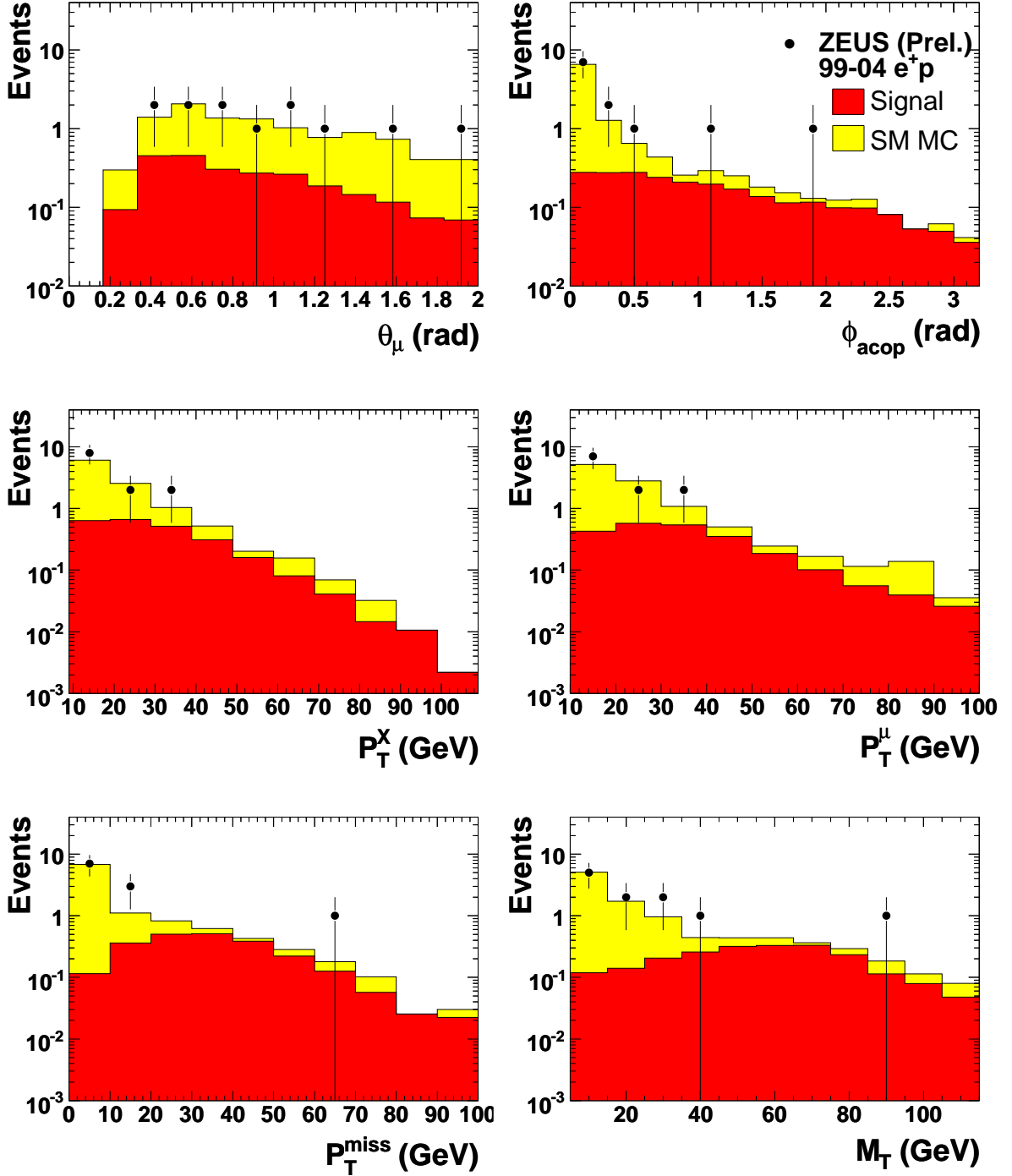


Figure 8: Isolated muon data (points) compared to absolutely-normalised Monte Carlo for the 1999-2000, 2003-04 e^+p running period after the initial event selection. Other details as in Fig. 5.

ZEUS

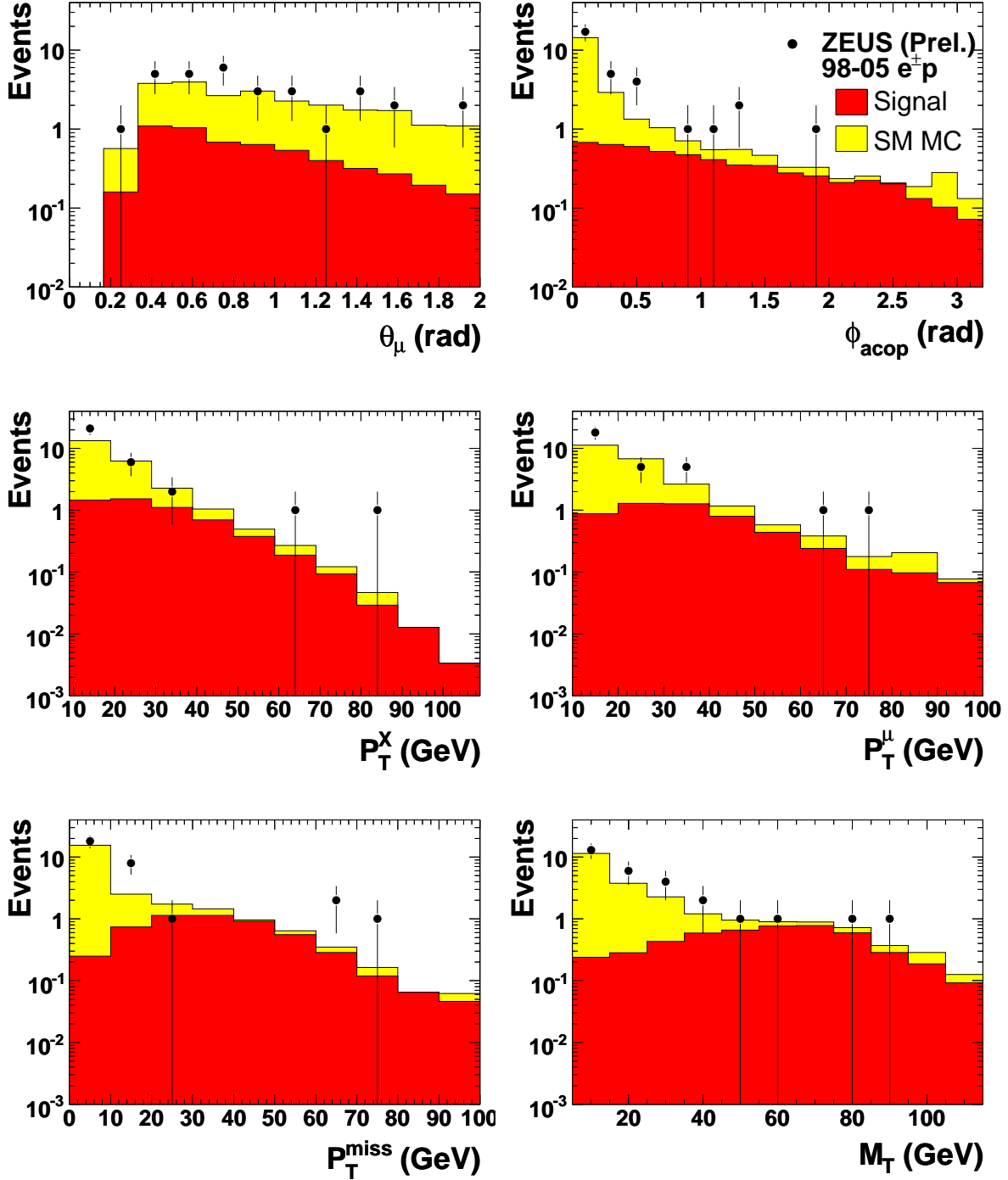


Figure 9: Isolated muon data (points) compared to absolutely-normalised Monte Carlo for the 1998-2005 $e^\pm p$ running period after the initial event selection. Other details as in Fig. 5.

ZEUS

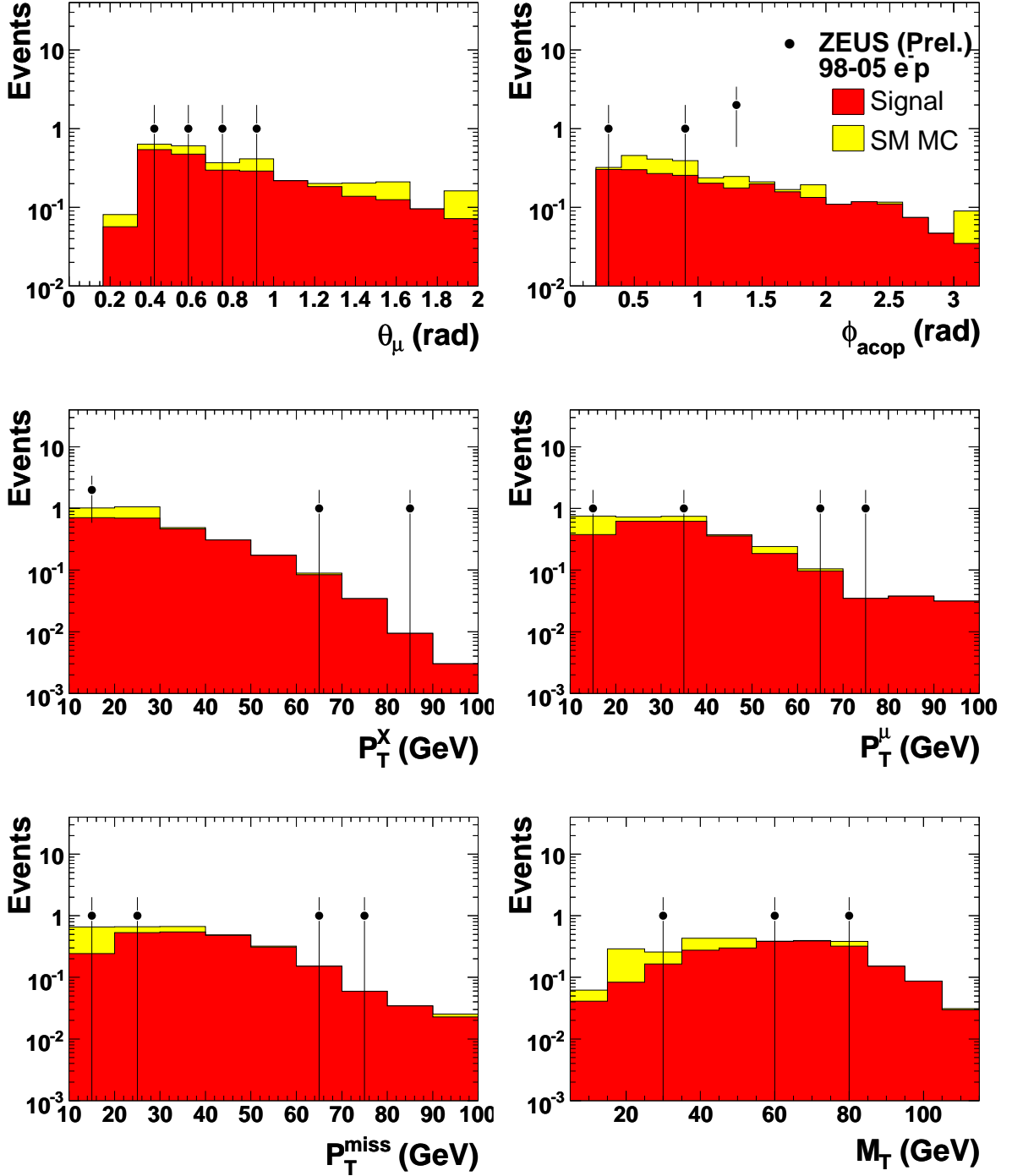


Figure 10: Isolated muon data (points) compared to absolutely-normalised Monte Carlo for the 1998-99, 2004-05 e^-p running period after the final event selection. Other details as in Fig. 5.

ZEUS

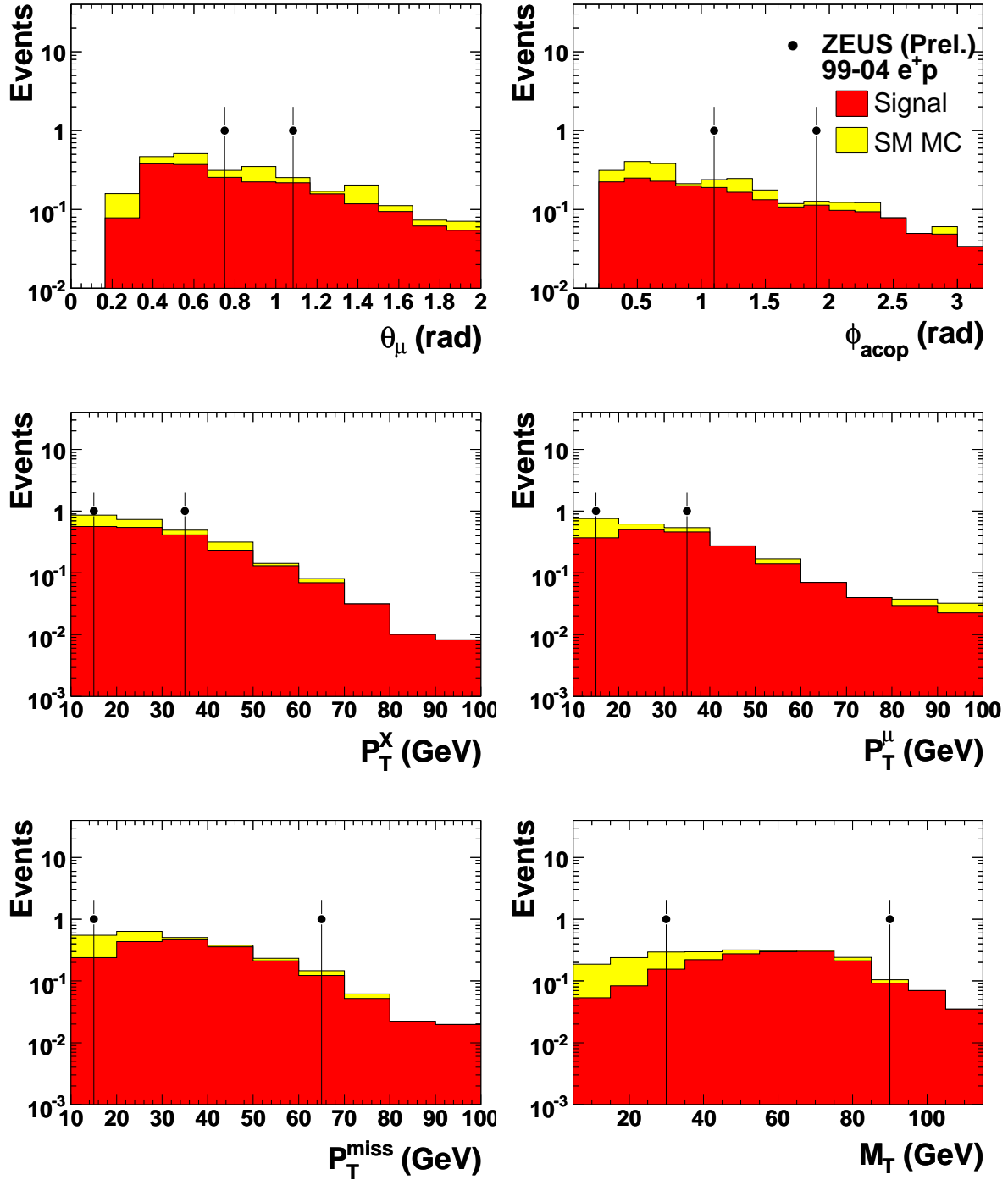


Figure 11: Isolated muon data (points) compared to absolutely-normalised Monte Carlo for the 1999-2000, 2003-04 e^+p running period after the final event selection. Other details as in Fig. 5.

ZEUS

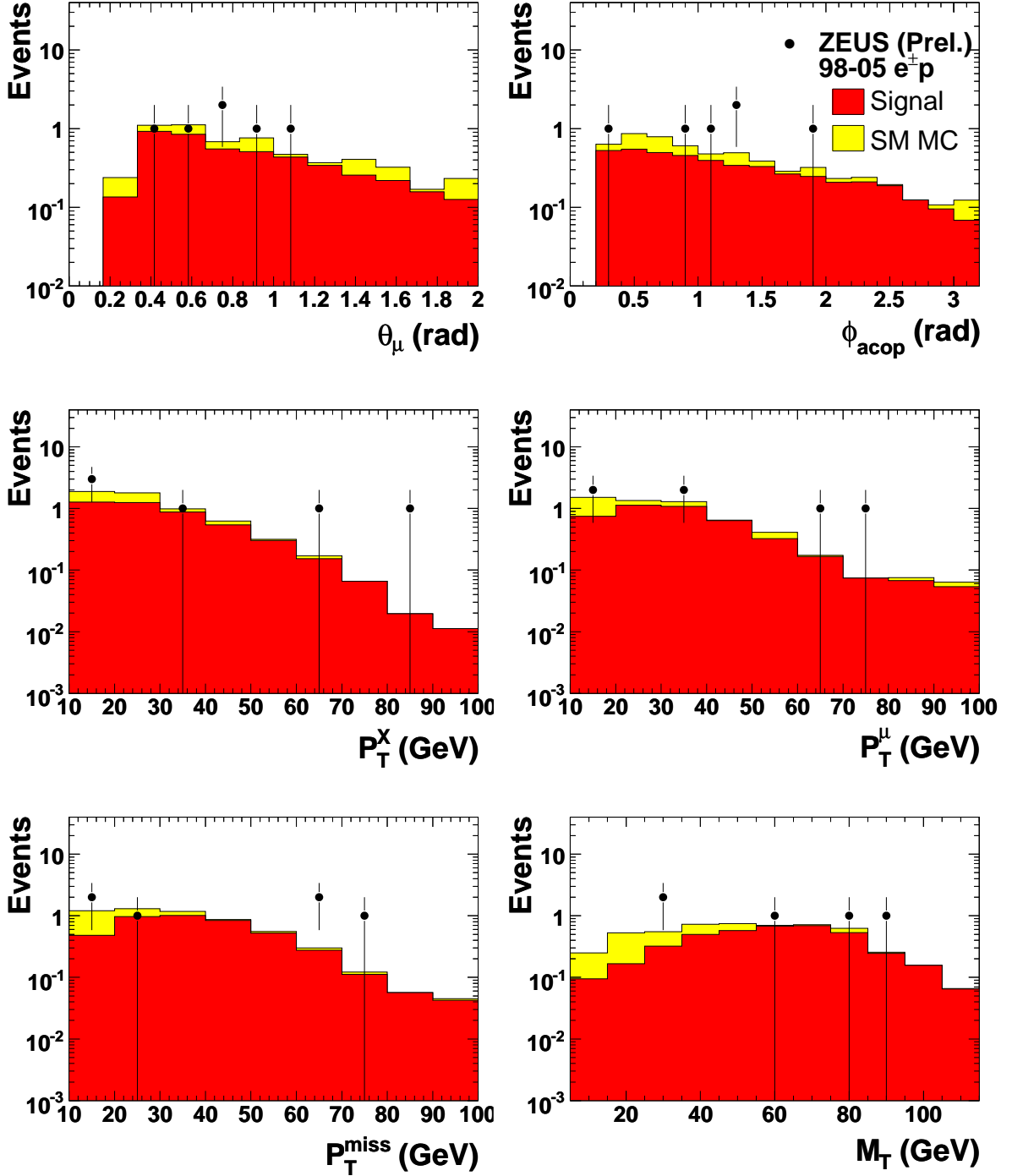


Figure 12: Isolated muon data (points) compared to absolutely-normalised Monte Carlo for the 1998-2005 $e^\pm p$ running period after the final event selection. Other details as in Fig. 5.

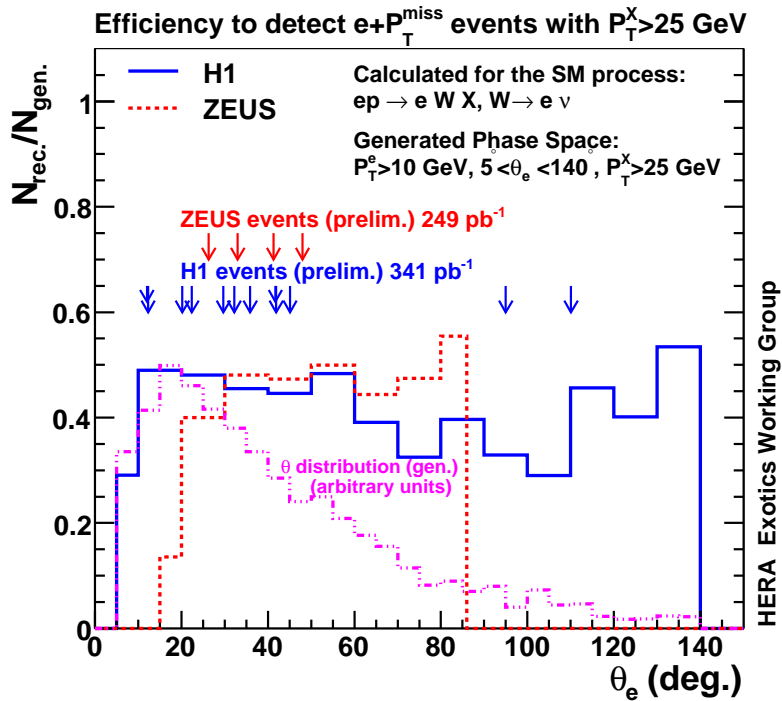
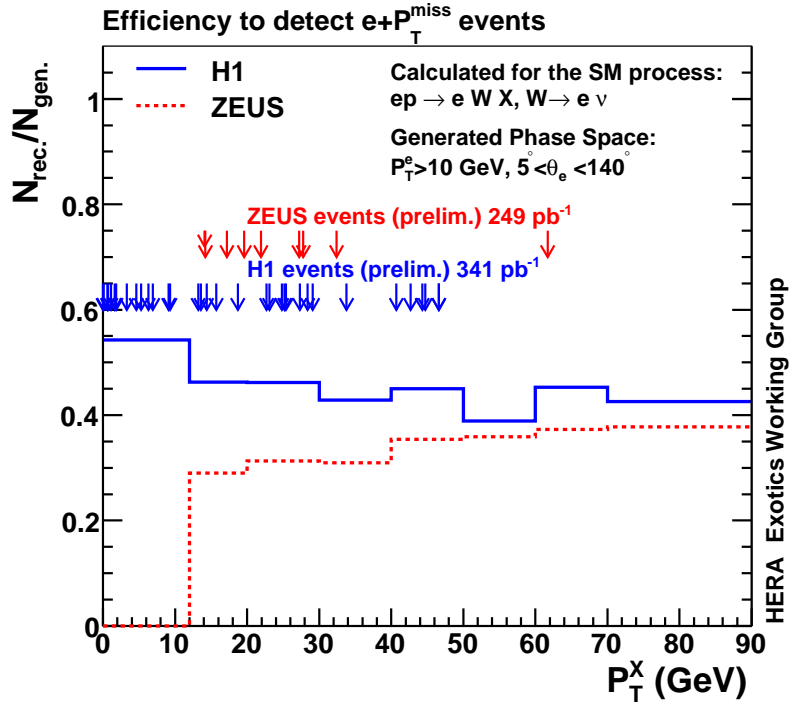


Figure 13: Comparison between the efficiencies of H1 and ZEUS for reconstructing $W \rightarrow e\nu$ events generated by EPVEC.

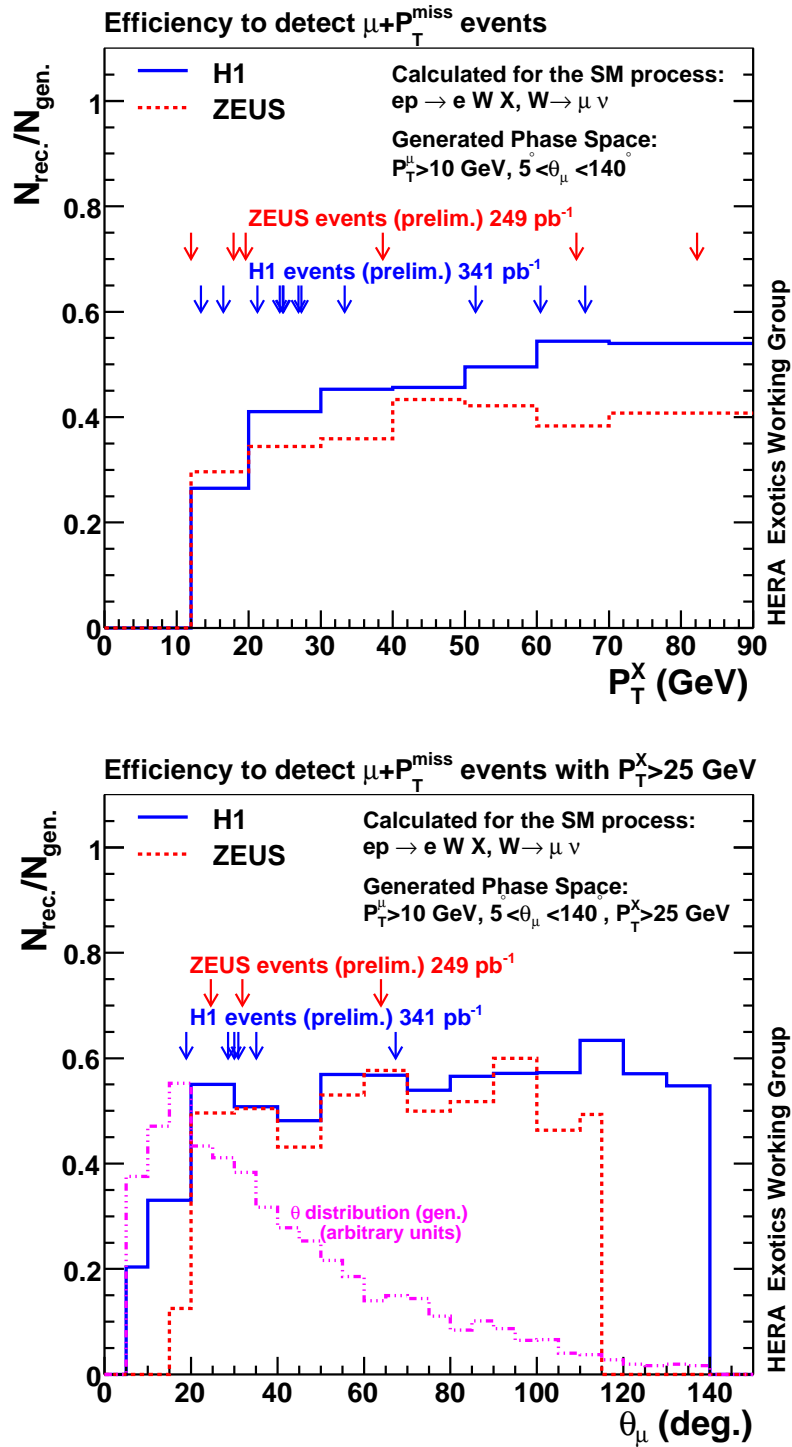


Figure 14: Comparison between the efficiencies of H1 and ZEUS for reconstructing $W \rightarrow \mu \nu$ events generated by EPVEC.